ISSN 0016-7932, Geomagnetism and Aeronomy, 2023, Vol. 63, No. 3, pp. 288–299. © Pleiades Publishing, Ltd., 2023.
Russian Text © The Author(s), 2023, published in Geomagnetizm i Aeronomiya, 2023, Vol. 63, No. 3, pp. 327–339.

Features of Polar Substorms: An Analysis of Individual Events

N. G. Kleimenova[a], *, L. I. Gromova[b], **, I. B. Despirak[c], L. M. Malysheva[a], S. V. Gromov[b], and A. A. Lyubchich[c]

[a] *Institute of Physics of the Earth, Russian Academy of Sciences (IPE RAS), Moscow, 123995 Russia*
[b] *Pushkov Institute of Terrestrial Magnetism, Ionosphere, and Radio Wave Propagation, Russian Academy of Sciences (IZMIRAN), Moscow, Troitsk, 142191 Russia*
[c] *Polar Geophysical Institute, Apatity, Murmansk region, 184209 Russia*
**e-mail: ngk1935@yandex.ru*
***e-mail: gromova@izmiran.ru*

Received January 12, 2023; revised January 18, 2023; accepted January 26, 2023

Abstract—Polar substorms include substorms observed at geomagnetic latitudes above 70° MLAT in the absence of simultaneous negative magnetic bays at lower latitudes, that is, substorms on the compressed contracted auroral oval. The general morphological features of polar substorms are considered based on the example of individual events registered on Svalbard arch. It is shown that polar substorms, like "classical" substorms, are characterized by the formation of a substorm current wedge and a steplike movement to the pole after the onset of a substorm, generation of *Pi*2 geomagnetic pulsations, and an increase of the *PC*-index of the polar cap before the onset of the substorm. At the same time, there are certain differences between polar substorms and "classical" substorms; namely, they start on more distant L-shells, develop in the region of a contracted auroral oval, occur at earlier pre-midnight hours, and generate only at low solar wind speeds and weakly disturbed geomagnetic conditions. It has been suggested that polar substorms may be a specific type of "classical" substorms that develop in the evening sector under magnetically quiet or weakly disturbed conditions when the auroral oval is concracted. The source of polar substorms may also be a local intensification of previously existing substorms in the post-midnight sector.

DOI: 10.1134/S0016793223600042

1. INTRODUCTION

Magnetospheric substorms are an important element of space weather; therefore, they have been intensively studied in the last 50 years. The energy entering from the solar wind into the growth phase of a substorm accumulates in the magnetosphere and its tail; then, during the substorm expantion phase, also called the "active phase," it is released explosively. At the same time, field-aligned currents and the ionospheric currents caused by them, which are observed on the Earth's surface in the form of bay-like perturbations of the geomagnetic field, increase in the magnetosphere, auroras flare up, geomagnetic pulsations and VLF emissions are generated, the precipitation of energetic particles into the ionosphere intensifies, etc.

The concept of a magnetospheric substorm was proposed in (Akasofu et al., 1964) as a complex of phenomena and processes covering almost the entire magnetosphere. In what follows, we will call such substorms "classical." Hundreds of publications have been devoted to the study of various geophysical manifestations of a substorm and their physics, but there is still no final answer to the question of what the source of a substorm is and where it is located. A magnetospheric substorm is a typical night disturbance in the region of the auroral oval (Feldshtein, 1963), i.e., in the region of development of discrete forms of auroras, which, depending on magnetic activity, can be located at geomagnetic latitudes from ~60° to ~75° MLAT and higher. As geomagnetic activity decreases, the oval shrinks and shifts poleward (Feldstein and Starkov, 1967). It has been reliably established that a substorm begins with a sudden brightening of a quiet arc near the equatorial boundary of the oval. Depending on the position of this boundary, the auroral oval is considered "normal," if this boundary is located in the interval 65°–66° MLAT; it is "expanded" if the boundary is below 65° MLAT and "contracted" if it is above 66° MLAT (Lui et al., 1973).

The polar boundary of the auroral oval coincides with the boundary of the closed magnetosphere; with the ionospheric projection of the boundary of open and closed field lines, which is the boundary of the polar cap. On the DMSP satellite, the polar boundary of the auroral oval was determined as the boundary of *b5i* and *b5e* particle precipitation (Newell et al., 1996). It was shown in (Clausen et al., 2012) that the latitude of the position of the maximum intensity of high-latitude field-aligned currents in the zone *R*1 (Iijima and

Potemra, 1978) is approximately 1° equatorial from the polar cap boundary and the low-latitude zone of field-aligned *R*2 currents localized near the equatorial boundary of the oval. In (Clausen et al., 2012), the position of the intensity maxima of *R*1 and *R*2 field-aligned currents were determined from magnetic observations at ionospheric heights (~780 km) in the AMPERE project (*Active Magnetosphere and Planetary Electrodynamics Response Experiment*), including simultaneous registration on 66 communication satellites.

During magnetically disturbed periods at high solar wind speeds, substorms can propagate to very high latitudes and be observed on the Earth's surface almost to the geomagnetic pole, for example, (Sergeev et al., 1979; Loomer and Gupta, 1980; Nielsen et al., 1988; Mende et al., 1999; Despirak et al., 2008). In this case, the higher the solar wind speed is, the greater the latitude is to which the substorm propagates (Dmitrieva and Sergeev, 1984). These are the so-called "extended" substorms (Despirak et al., 2008; Despirak et al., 2018) or "substorms on an extended oval."

At the same time, it was found that at such high latitudes substorms can also be observed during magnetically quiet times when the auroral oval is contracted and its equatorial boundary is marked at geomagnetic latitudes above 66° MLAT. These substorms have been called "substorms on a contracted oval" (Akasofu et al., 1973; Lui et al., 1976; Milan et al., 2008), such substorms were later called "polar substorms" (Kleimenova et al., 2012; Despirak and others. 2014, 2022; Safargaleev et al., 2018; Safargaleev et al., 2020), since they are observed near the polar boundary of the oval. Studies of these substorms as a specific type of classical substorms are obviously insufficient and, in fact, are just beginning.

It was established (Kleimenova et al., 2012) that polar substorms are observed in the pre-midnight hours (20–22 MLT) with weak geomagnetic activity ($Kp \sim 2$), most often in the late recovery phase of a magnetic storm and are accompanied by intense geomagnetic pulsations in the *Pi*2 and *Pi*3 range, exceeding the typical amplitude of these pulsations at auroral latitudes by more than an order of magnitude. Under favorable weather conditions during polar substorms, auroras are recorded in the form of arcs elongated along an oval, sometimes with unusual spiral structures. During the explosive phase of a substorm, the arcs quickly move poleward, which was confirmed in (Safargaleev et al., 2020; Despirak et al., 2022). It was established in (Despirak et al., 2014, 2019; Despirak et al., 2018) that polar substorms are recorded at low solar wind speed observed after the passage of a high-velocity recurrent flow, or during a slow solar wind flow, as well as in the late recovery phase of a geomagnetic storm.

The purpose of this work is to continue the study of polar substorms in order to reveal their differences (or similarities) from the morphological characteristics of "classical" substorms.

1. OBSERVATION RESULTS

This work is based on an analysis of observations on the Scandinavian meridian of the IMAGE magnetometer network (http://space.fmi.fi/image/) with a cadence of 10 s. This is the world's only dense network of stations located almost along the geomagnetic meridian (~105°–110° MLON, with MLT = UT + 2.5 h) from the polar latitudes of the Spitsbergen archipelago to the middle latitudes of Belarus. We considered observational data for the winter months (November–February), when auroras are recorded, the 24th cycle of solar activity, from 2010 to 2021.

We referred to polar substorms the substorms that were recorded in Svalbard at geomagnetic latitudes above 70° MLAT in the absence of negative magnetic bays at lower latitudes, i.e., at mainland stations. In Figure 1a a geographical map of Scandinavia is shown, indicating the IMAGE stations used in this work. The map shows that the intermediate station between the Svalbard archipelago and the mainland is the Bear Island station (BJN, 71.4° MLAT) on Bear Island, to the south of which there is a sea, on the coast of which the first continental Soeroeya station is located (SOR, 67.8° MLAT). If magnetic bays were observed at BJN but were absent at SOR, then the mid-distance between the BJN and SOR sites can be considered as a conditional low-latitude boundary of the appearance of magnetic bays; about 70° MLAT; therefore, this latitude was used as the boundary latitude in the development of polar substorms. This corresponds to the conditions of a contracted oval (Lui et al., 1973). In Figure 1b the typical position of the auroral oval during the development of a polar substorm is given, which will be considered in detail below.

For further analysis, 290 cases of polar substorms recorded in Svalbard were selected. An analysis of the diurnal variation of their occurrence showed that the vast majority (82%) of the events were observed before the geomagnetic midnight.

2.1. The Diurnal Variation of the Onset of Polar Substorms

One important characteristic of a substorm is the time and location of its abrupt onset; these studies are important for solving the problem of the nature and mechanism of the onset of a substorm (Frey et al., 2004). On the Earth's surface, the beginning of a substorm is determined by the time of a sudden sharp decrease in the *X*-components of the magnetic field at the lowest latitude station of the appearance of the substorm. In the studied events, as a rule, this was the BJN station.

In (Milan et al., 2010), data on the local magnetic time (MLT) of the onsets of about 2000 isolated sub-

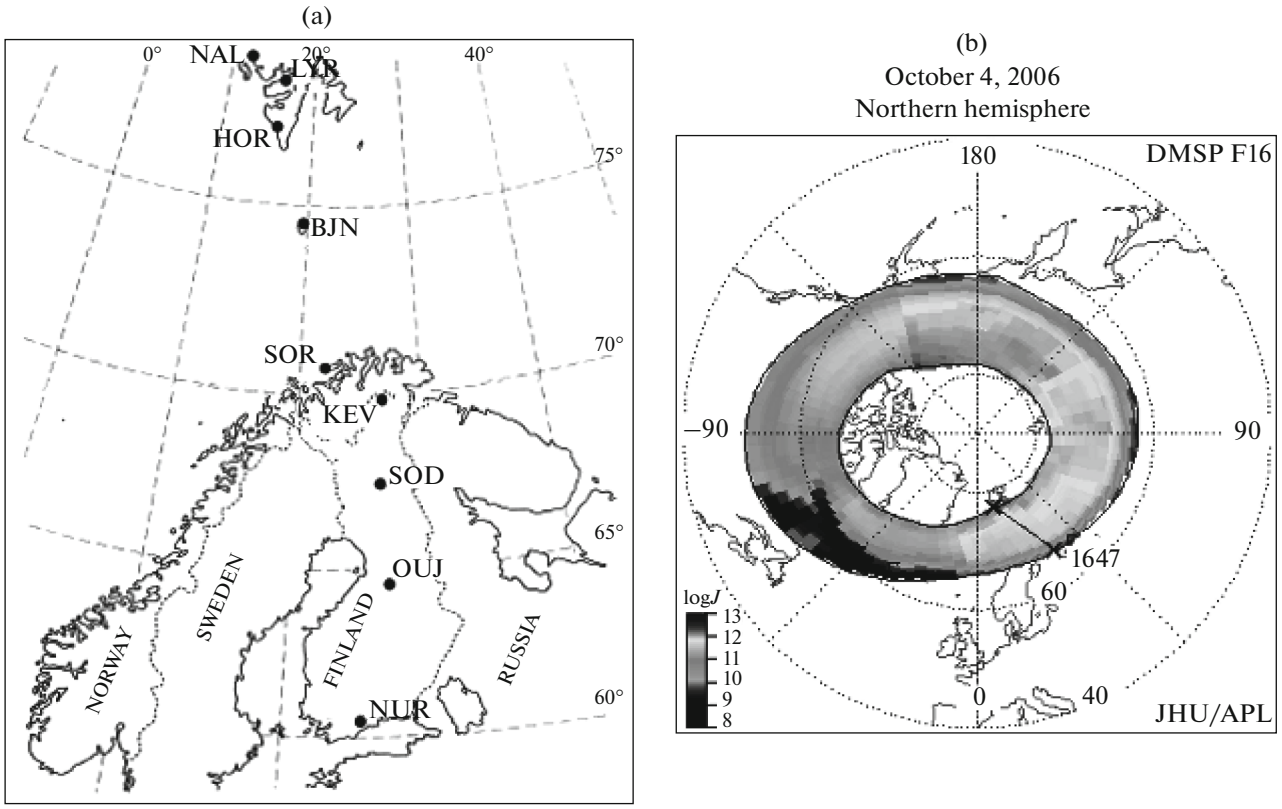

Fig. 1. A geographic map of used stations of the IMAGE profile (a) and the position of the auroral oval on October 4, 2006 (b).

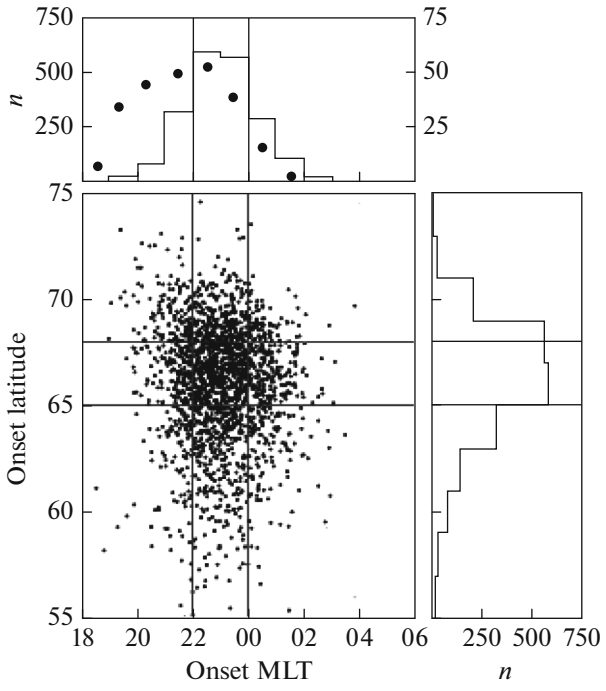

Fig. 2. The diurnal variation of substorm onsets from (Milan et al., 2010). Bold dots show the diurnal variation obtained by us for the onset of polar substorms recorded at arch. Svalbard.

storms were recorded on the IMAGE satellite (Mende et al., 2000) in 2000–2002 (Frey et al., 2004). Figure 2 shows the results obtained in (Milan et al., 2010). In this work, substorms were chosen according to very strict criteria: only isolated substorms were studied, their onsets were accompanied by a local brightening of the auroras, which then rapidly moved poleward and westward, into the evening sector. Figure 2 shows the point cloud of substorm onsets obtained in (Milan et al., 2010) relative to the MLT and geomagnetic latitude, while the upper and right graphs show the same distribution by the number of cases (n). On the upper graph, we plotted the distribution of polar substorm onsets we obtained in Svalbard (numbers on the right scale) with thick dots.

Figure 2 shows that the majority of substorms that can be attributed to "classical" substorms begin at geomagnetic latitudes of 65°–67° MLAT (i.e., on the "normal" oval according to (Lui et al., 1973) 22–24 MLT. Most of the substorms we studied began near BJN; at higher geomagnetic latitudes, at about 70° MLAT, in the range of 20–23 MLT. In general terms, this agrees with the plot (Milan et al., 2010) of the location of substorm onsets at such latitudes (upper left corner of the distribution cloud in Fig. 2). Thus, in contrast to "classical" substorms, the onset of polar substorms is observed in the evening sector and at higher latitudes.

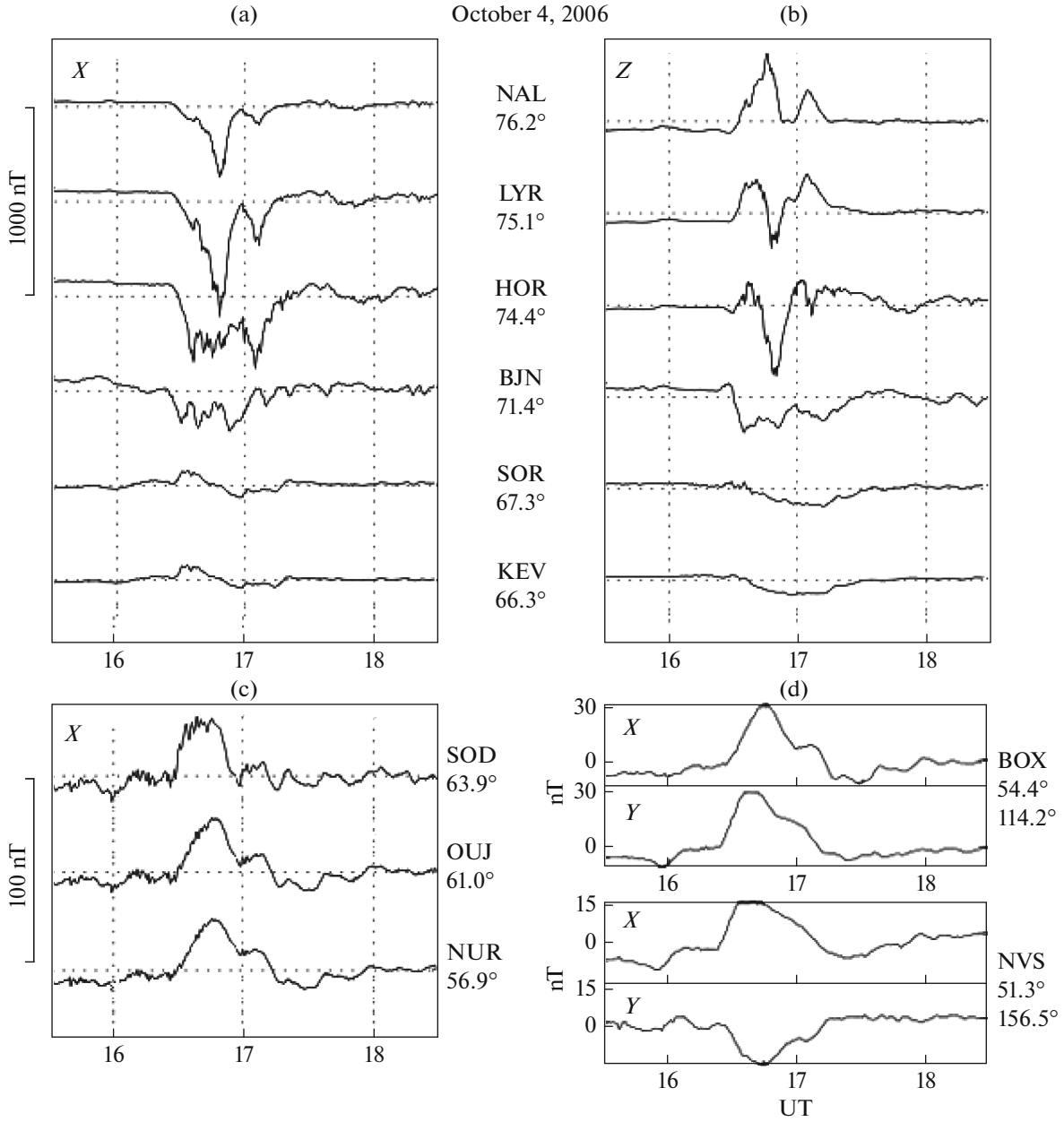

Fig. 3. High-latitude magnetograms (a, b) and subauroral (c) IMAGE profile stations for the October 4, 2006 polar substorm event; (d) magnetograms of low-latitude stations Borok (BOX) and Novosibirsk (NVS).

2.2. The Polar Substorm on October 4, 2006

For a detailed analysis of individual events, we chose the polar substorm recorded on Svalbard on October 4, 2006 at 1630–1730 UT, since during this time we found the position of the auroral oval in geographic coordinates in our archives (Fig. 1b) determined by the OVATION program, which is currently closed. One feature of this event was that in this time interval the position of the oval was determined from the data of observations of particle precipitation on the DMSP F16 satellite flying over Svalbard. The positions of the auroral oval in other sectors of the local time were plotted using model calculations. Unfortunately, the DMSP satellite site does not provide registration results for flights later than 1500 UT (the flyby we were interested in was at 1647 UT).

In Figures 3a, 3b magnetograms of high-latitude IMAGE stations are presented. It can be seen that the polar substorm began at about 1630 UT between the BJN and HOR stations. Comparing this with the position of the auroral oval (Fig. 1b), we can conclude that, unlike the "classical" substorms that begin near the equatorial boundary of the oval, this polar substorm began and developed at higher latitudes closer to

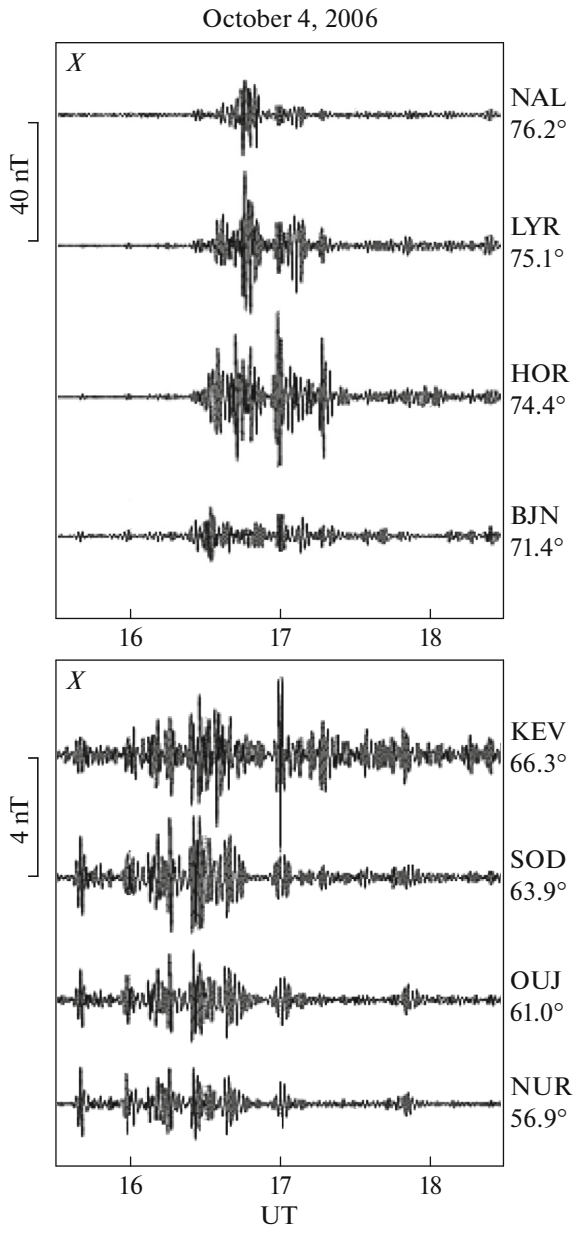

Fig. 4. *Pi*2 geomagnetic range pulsations at IMAGE profile stations on October 4, 2006.

the polar boundary of the oval. The same development of a polar substorm was noted in (Safargaleev et al., 2020).

Meteorological conditions on Svalbard that day did not allow observations of the auroras. We note that in the vicinity of BJN there are no all-sky cameras (ASCs) for recording auroras. The nearest continental station where such observations are made, Abisko (ABK) is about 800 km south of BJN. Usually, if the onset of a polar substorm was recorded near BJN, then in good weather conditions, in the uppermost viewing angle of the ASC camera in ABK, one could see the appearance of a glow corresponding to an aurora breakup in BJN.

Figure 3c shows that the discussed polar substorm, like the "classical" substorm, was accompanied by the development of a positive magnetic bay at lower latitudes. This indicates the formation of a substorm current wedge (SCW) (McPherron et al., 1973; Sergeyev, 1974; Horning et al., 1974) centered on the substorm start meridian, i.e., the development of a three-dimensional current system, whose generation mechanisms were considered in detail, for example, in the review paper (Kepko et al., 2015). The longitude dimensions of the SCW ionospheric projection area can be determined from the sign of *Y*-components of the magnetic field at mid-latitude stations. In Figure 3g magnetograms of mid-latitude Borok stations (BOX, 54.4° MLAT, 114° MLON) located near the meridian of the IMAGE network and Novosibirsk station (NVS, 51.3° MLAT, 156° MLON) are shown. It can be seen that the sign of variations in *Y*-components of the field at these stations had the opposite direction. Consequently, the center of the substorm current wedge, i.e., the onset region of the considered polar substorm was located between these stations, to the east of the Scandinavian IMAGE meridian.

Small positive field deviations are visible on the magnetograms of subauroral and midlatitude stations even before the onset of a substorm, which, according to (Troshichev et al., 1974), may be the result of an increase in the eastern electrojet in the evening sector due to an increase in magnetospheric convection in the growth phase of a substorm.

Let us consider the features of geomagnetic pulsations typical for the onset of a substorm in the *Pi*2 range (periods of 40–150 s), whose characteristics have been discussed in many articles and reviews, for example, (Saito, 1969; Troitskaya and Kleimenova, 1972; Pudovkin et al., 1976; Pashin et al., 1982; Olson, 1999; Keiling and Takahasi, 2011). Figure 4 shows the *X*-component of the *Pi*2 geomagnetic pulsation range during this substorm obtained by filtering 10-s magnetograms in the 7–20 MHz frequency band. The upper plot in Fig. 4 shows the pulsations at higher latitude stations of the IMAGE profile, while the lower plot shows pulsations at lower latitude stations (the geomagnetic latitude of each station is given to the right of the magnetogram, under the station code). The scale of the upper and lower graphs differs by 10 times. It can be seen that, as in the case of "classical" substorms, the onset of a polar substorm and each of its activations were accompanied at high latitudes by a burst of *Pi*2 geomagnetic pulsations, whose amplitude reached 40–50 nT, i.e., it was an order of magnitude higher than the typical amplitudes *Pi*2 pulsations. This feature of high-latitude *Pi*2 pulsations during polar substorms was previously noted in (Kleimenova et al., 2012). The start of the *Pi*2 burst moved poleward with

time, synchronously with the onset of a polar substorm, which is also typical of a "classical" substorm.

As follows from the magnetograms in Fig. 3, at 1700 UT a new, weaker substorm began in HOR with a maximum intensity in HOR. In geomagnetic pulsations (Fig. 4), the beginning of this substorm manifested itself as a short but very intense *Pi*2 burst, which is coherent at all latitudes (most clearly seen at lower latitude stations), which is typical of a "classical" substorm.

Separate coherent bursts of *Pi*2 pulsations in subauroral latitudes with an amplitude of up to 3 nT were also observed before the polar substorm (lower graph in Fig. 4), in its growth phase, which is also typical of a "classical" substorm, for example, (Zverev et al., 1969). These pulsations are almost invisible in the top graph due to the relatively coarse vertical scale.

Thus, the behavior of *Pi*2 geomagnetic pulsations during the development of a polar substorm is the same as in the case of a "classical" substorm, but in contrast to the "classical" substorm, the amplitudes of high-latitude *Pi*2 pulsations during a polar substorm are almost an order of magnitude higher.

2.3. The Polar Substorm on December 17, 2013

As an example, let us consider one more case of a polar substorm recorded in later years (December 17, 2013), when there were observational data from the AMPERE project (Anderson et al., 2002). As in the previous case, this polar substorm was observed during a relatively magnetically quiet time ($Kp = 1–2$). In our work, we used the publicly available data of the AMPERE project presented on the website (https://ampere.jhuapl.edu/browse/) in the form of maps of the distribution of ionospheric currents generalized over 10 min, constructed based on the results of a spherical harmonic analysis of magnetic measurements on 66 simultaneously operating ionospheric satellites. Based on these measurements, maps of the distribution of field-aligned currents flowing into and flowing out of the ionosphere are also calculated. In our work, maps of field-aligned currents are not given, since the downward and upward currents are shown on them in blue and red, which, unfortunately, become indistinguishable when converted to black and white.

Figure 5 shows magnetograms of the same IMAGE stations as in Fig. 3 in the same format. The polar substorm started at about 1820 UT between the BJN and SOR stations, closer to BJN. The substorm then began to rapidly move poleward. The maximum intensity of the substorm was first noted in the HOR, and the ionospheric current, judging by the variations Z-components of the field, was below the HOR, but then quickly moved to higher latitudes. The intensity of this polar substorm was almost half that of the October 4, 2006 polar substorm (Fig. 3).

As in the event of October 4, 2006 considered above, in the case of the polar substorm on December 17, 2013, a positive magnetic bay was observed at subauroral and middle latitudes, whose peak was at SOD at first and coincided with the maximum of the substorm at BJN. It is interesting to note that the magnitude of the positive peak at SOD, corresponding to the substorm maximum at BJN, is also seen at the lower latitude OUJ and NUR stations (Fig. 5) with an amplitude rapidly decreasing with latitude. The next gentle maximum of the subauroral positive bay coincided with the maximum of the substorm in the HOR and is clearly visible at all three stations (SOD, OUJ, and NUR) with a close amplitude. Variations in the X- and Y-component of the field at the low-latitude BOX and NVS stations indicate that the center of the current wedge of this polar substorm, as in the previous case, was located east of the IMAGE meridian.

As in the previous event, before the onset of the substorm at subauroral and midlatitude stations, small positive deviations were observed in the X-component of the field (Fig. 5), indicating an increase in the eastern electrojet in the evening sector in the growth phase of the substorm. It can be seen that the amplitude of these deviations decreased with decreasing latitude. Such variations are typical for a "classical" substorm, for example, (Troshichev et al., 1974).

*Pi*2 geomagnetic pulsations accompanying this substorm are shown in Fig. 6. The general regularities of the dynamics of geomagnetic pulsations were similar to the event of October 4, 2006. However, at high latitude stations, the *Pi*2 amplitude, as well as the disturbances of the magnetic field on December 17, 2013, was less than in the event of October 4, 2006. This means that the generation of pulsations at high latitudes is somehow (it is not clear how) related to the intensity of the ionospheric current or to the conductivity ionosphere. It is interesting to note that the reverse pattern was observed at low latitudes. The *Pi*2 ripple amplitude at KEV and SOD on December 17, 2013 was significantly larger than that of October 4, 2006 (see the difference in the vertical scale in Figs. 4 and 6). The *Pi*2 pulsations in the growth phase for the substorms on December 17, 2013 were also much more intense. This fact has not been explained.

Figure 7 shows two AMPERE maps of the distribution of ionospheric currents before the onset of a polar substorm, i.e., during its growth phase (about 1800 UT) and during the onset of this substorm (at 1825 UT). It can be seen that before this substorm in the evening sector, an easterly electrojet was observed, whose strengthening is noted at the subauroral IMAGE stations (Fig. 5). In the morning sector (~02–09 MLT), an increase in the western electrojet was noted, which manifested itself on the Earth's surface as the development of a magnetic substorm, clearly visible at ~04 MLT on the Tiksi station magnetograms, 66.7° MLAT (these data are not presented here).

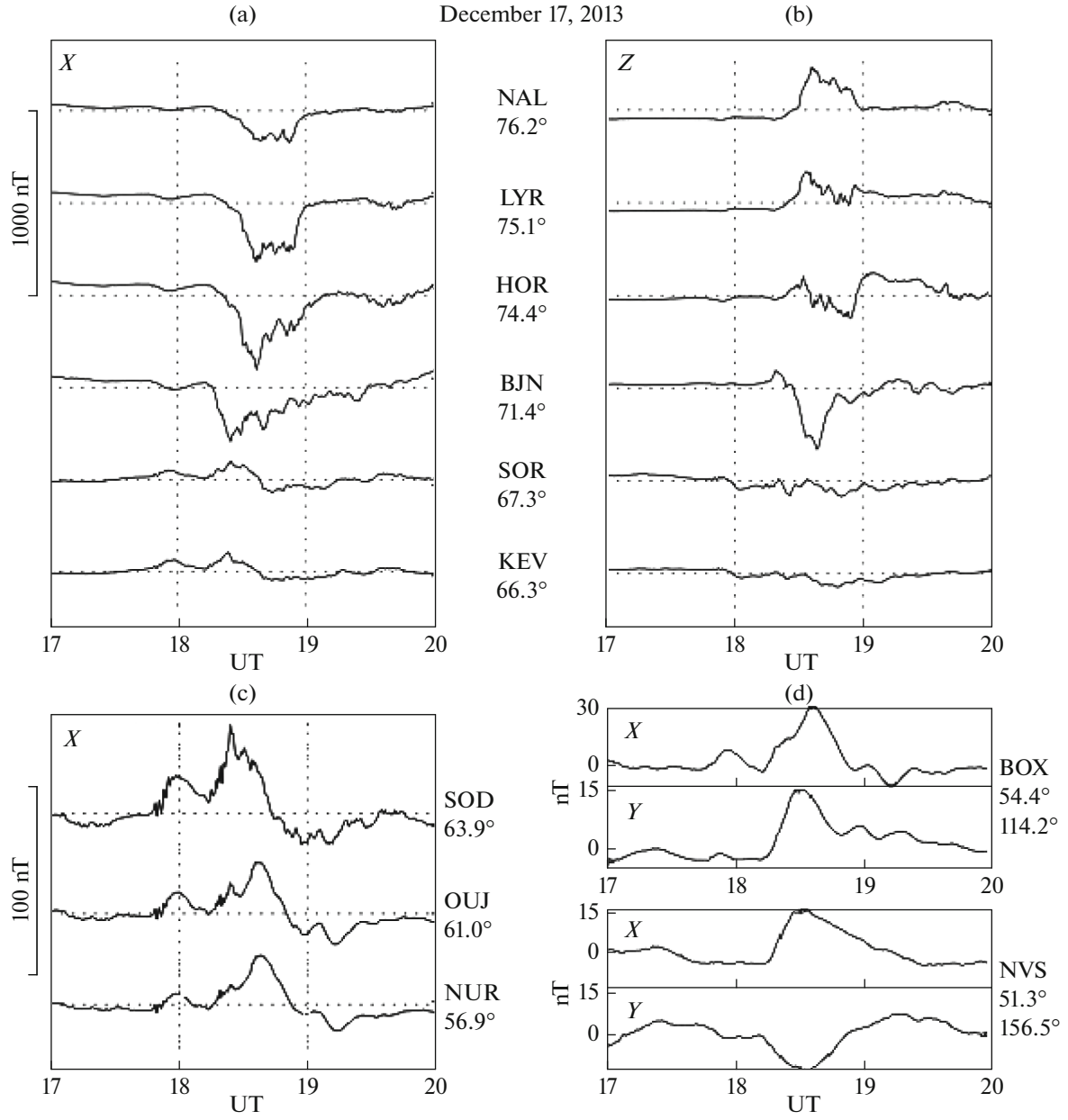

Fig. 5. The same as in Fig. 3, for the event on December 17, 2013.

The onset of the polar substorm was associated with the appearance of a strong vortex near Svalbard (right map in Fig. 7), indicating an increase in the field-aligned currents, which was also noted on the color maps of AMPERE field-aligned currents, which are not shown here. Near the local magnetic midnight in this region of space there is a boundary between the eastern (evening) and western (post-midnight) currents (the Harang discontinuity). In the subpolar latitudes of the evening sector, a fairly intense westward current developed, which was observed on the Earth's surface as a polar substorm in Svalbard. At the same time, an eastern electrojet is visible above the continental stations and a western electrojet is visible at higher latitudes.

Thus, the analyzed polar substorm is not a separate independent phenomenon, but is the result of the development of a high-latitude magnetic disturbance in the evening sector as a local intensification of an earlier substorm in the post-midnight sector of the Earth.

2. DISCUSSION

Above, we presented the results of a detailed study of two substorms recorded at Svalbard arch. in a contracted oval. In both cases, disturbances were observed

on the IMAGE meridian only at high geomagnetic latitudes (>70° MLAT) in the absence of negative magnetic bays at lower latitudes, i.e., by definition (Kleimenova et al., 2012), both substorms can be classified as "polar substorms."

We note that in a number of early works, for example, (Hones et al., 1971, 1985), bay-like perturbations at subpolar latitudes were considered as a sudden movement of auroras and the western electrojet to high latitudes ("poleward leap"), or detached "clouds" field-aligned currents ("detached region"), (Iijima and Potemra, 1978). According to (Pytte et al., 1978) "poleward leap" appears in the late substorm recovery phase and is associated with the stretching of field lines in the magnetotail. The morphological characteristics of the "poleward leap" fundamentally differ from the characteristics of the high-latitude expansion of magnetospheric substorms (Pytte et al., 1978), primarily in the absence of *Pi*2 geomagnetic pulsations, which are a characteristic sign of the development of a substorm (Saito et al., 1976) and its activations, as well as the absence of substorm current wedge formation, i.e., the absence of positive magnetic bays at subauroral and middle latitudes. Consequently, the polar substorms considered in our work cannot be classified as disturbances of the "poleward leap" type.

Both considered substorms were observed during quiet space weather; there were no significant disturbances in the previous days. Under such conditions, the equatorial boundary of the auroral oval moves towards high latitudes; the oval becomes contracted to the polar cap. Figure 8 shows variations in the parameters of the interplanetary magnetic field (IMF) and solar wind (velocity and dynamic pressure) according to 1-min OMNI data (http://omniweb. gsfc.nasa.gov) during both considered polar substorms. It can be seen that the distinguishing feature of both events was the low solar wind speed (of the order of 400 km/s and lower), which led to a decrease in the size of the auroral oval (its compression towards the pole). Polar substorms were observed against the background of small but relatively long negative values *Bz* IMF that appeared about 6 hours before the first considered polar substorm and about 3 hours before the second. This led to an increase in magnetospheric convection and a corresponding increase in the eastern electrojet in the evening sector and the western electrojet in the morning sector. The PC polar cap index, which is an indicator of the level of transfer of solar wind energy to the Earth's magnetosphere (Troshichev et al., 2014), also began to increase almost 3 h before the onset of the polar substorm, which indicates an increase in the influx of solar wind energy into the magnetosphere, as was considered, for example, in (Troshichev and Janzhura, 2009; Troshichev et al., 2014).

The *AL* index during the first analyzed polar substorm (October 4, 2006) were almost 50% lower than

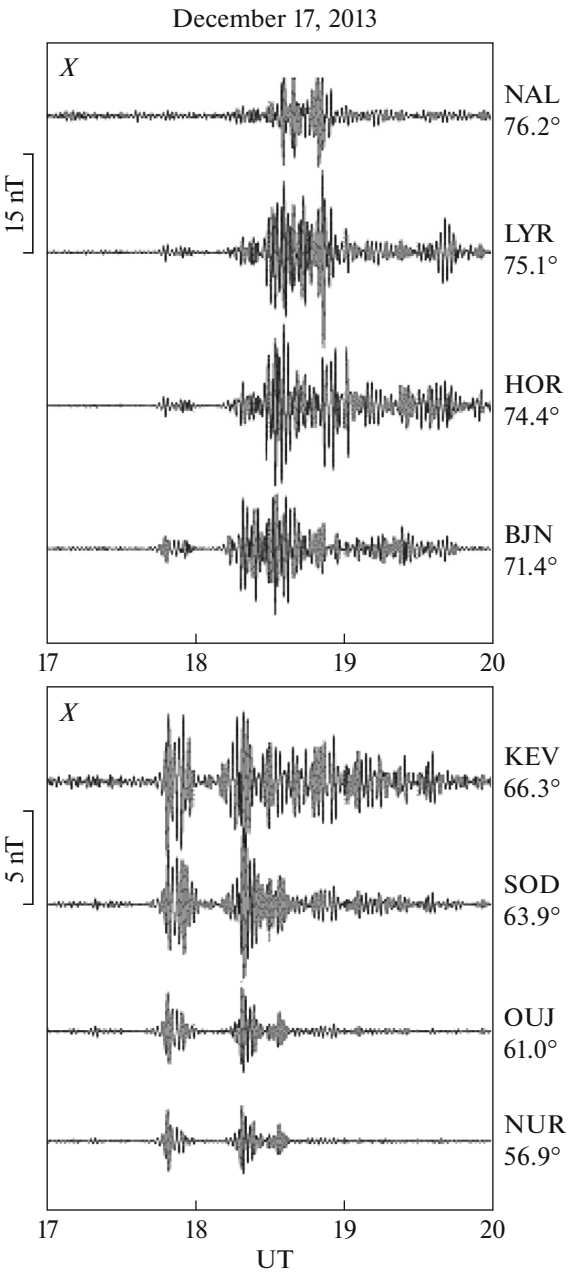

Fig. 6. The same as in Fig. 4, for the event on December 17, 2013.

during the second one (December 17, 2013); at the same time, the first polar substorm was almost twice as intense (about 600 nT) than the second one (about 300 nT). The high-latitude stations at which polar substorms were observed are not included in the set of stations, according to the observational data from the *AL*-index. The main contribution to the *AL*-index at 1800–2000 UT is made by observations at the Tiksi, Dikson, and Chelyuskin Russian auroral stations, which at that time are in the post-midnight sector of the Earth. An analysis of the magnetograms at these

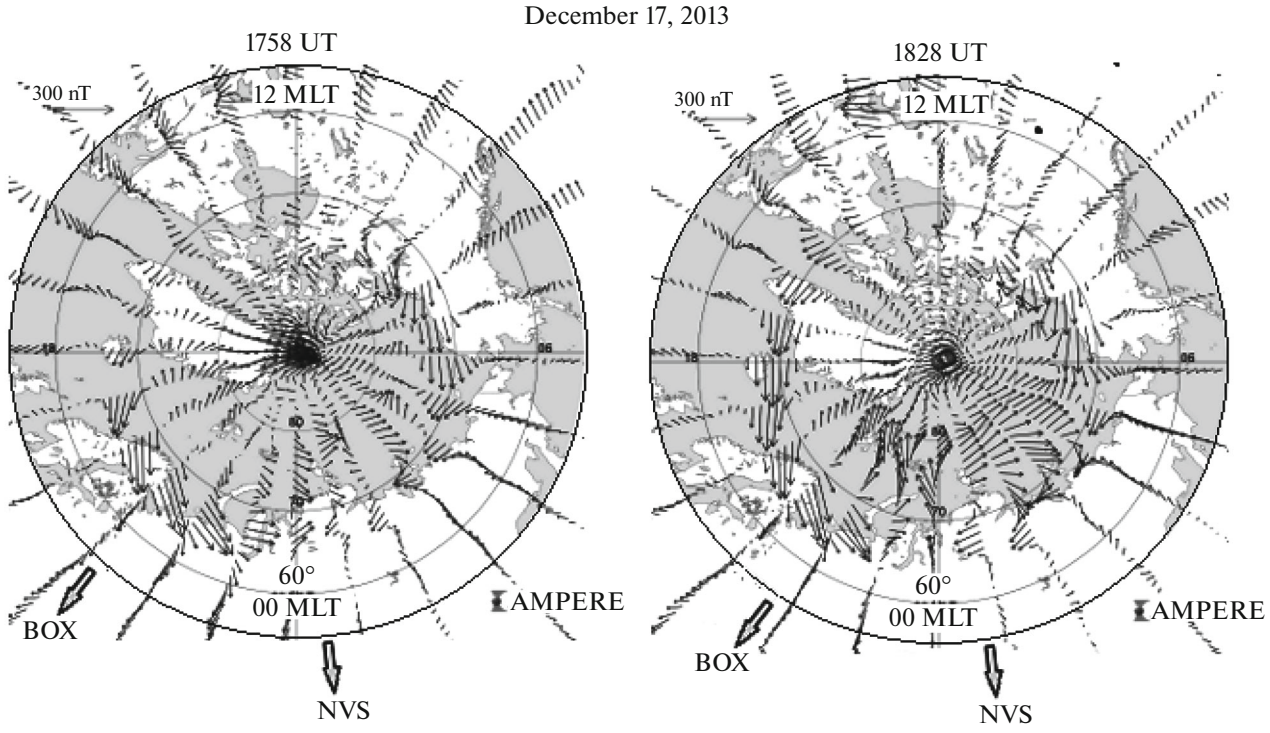

Fig. 7. AMPERE maps of ionospheric currents before and during the December 17, 2013 polar substorm.

stations showed that in both cases a substorm with an amplitude of about 200 nT was recorded at Tiksi, and on December 17, 2013, the most intense substorm (almost up to 400 nT) was observed at Dikson station (these magnetograms are not presented here, they can be found on the SuperMAG website (https://supermag.jhuapl.edu/). This led to an increased *AL*-index in the second case. It can also be concluded that the amplitude of the polar substorm in the evening sector does not depend on the amplitude of the substorm observed at this time in the post-midnight (morning) sector.

We note that, according to a number of researchers, including Akasofu (2017), the onset of generation of polar substorms, as well as "classical" substorms, is associated with processes inside the closed magnetosphere (rather than in its tail), and apparently occurs inside the plasma ring surrounding the Earth as the outer part of the ring current, as considered in (Antonova et al., 2015, 2016). During magnetically quiet times, field-aligned currents increase in this region of the magnetosphere due to the azimuthal plasma pressure (Antonova et al., 2023). The role of turbulence in this process is currently being actively discussed.

We found that the general patterns of development of polar substorms correspond to the typical characteristics of "classical" substorms, namely, the formation of a current wedge of a substorm (positive magnetic bays at lower latitudes), an abrupt movement of activations to the pole after the onset of a substorm, and the generation of *Pi*2 geomagnetic pulsations.

It is known that the onset of a "classical" substorm is defined as a sudden brightening of the equatorial quiet auroral arc itself, i.e., near the equatorial boundary of the auroral oval. Since polar substorms are observed on a compressed oval, it is not surprising that the equatorial boundary of the oval is located at higher latitudes than under typical conditions. This means that the source of the onset of excitation of polar substorms is located in the magnetosphere at more distant *L*-shells in the region of a weaker magnetic field, where there are probably less stringent conditions for the development of the corresponding instability; therefore, polar substorms are observed in weakly disturbed geomagnetic conditions and at low solar wind speeds.

3. CONCLUSIONS

We found that the general patterns of development of polar substorms correspond to the typical characteristics of "classical" substorms, namely, (1) the formation of a substorm current wedge (positive magnetic bays at lower latitudes); (2) abrupt movement of activations to the pole after the onset of a substorm; (3) generation of geomagnetic pulsations *Pi*2; and (4) an increase in the PC polar cap index before the onset of the substorm.

At the same time, it was established that there are certain differences between polar substorms and "classical" substorms, namely, (1) the development of nega-

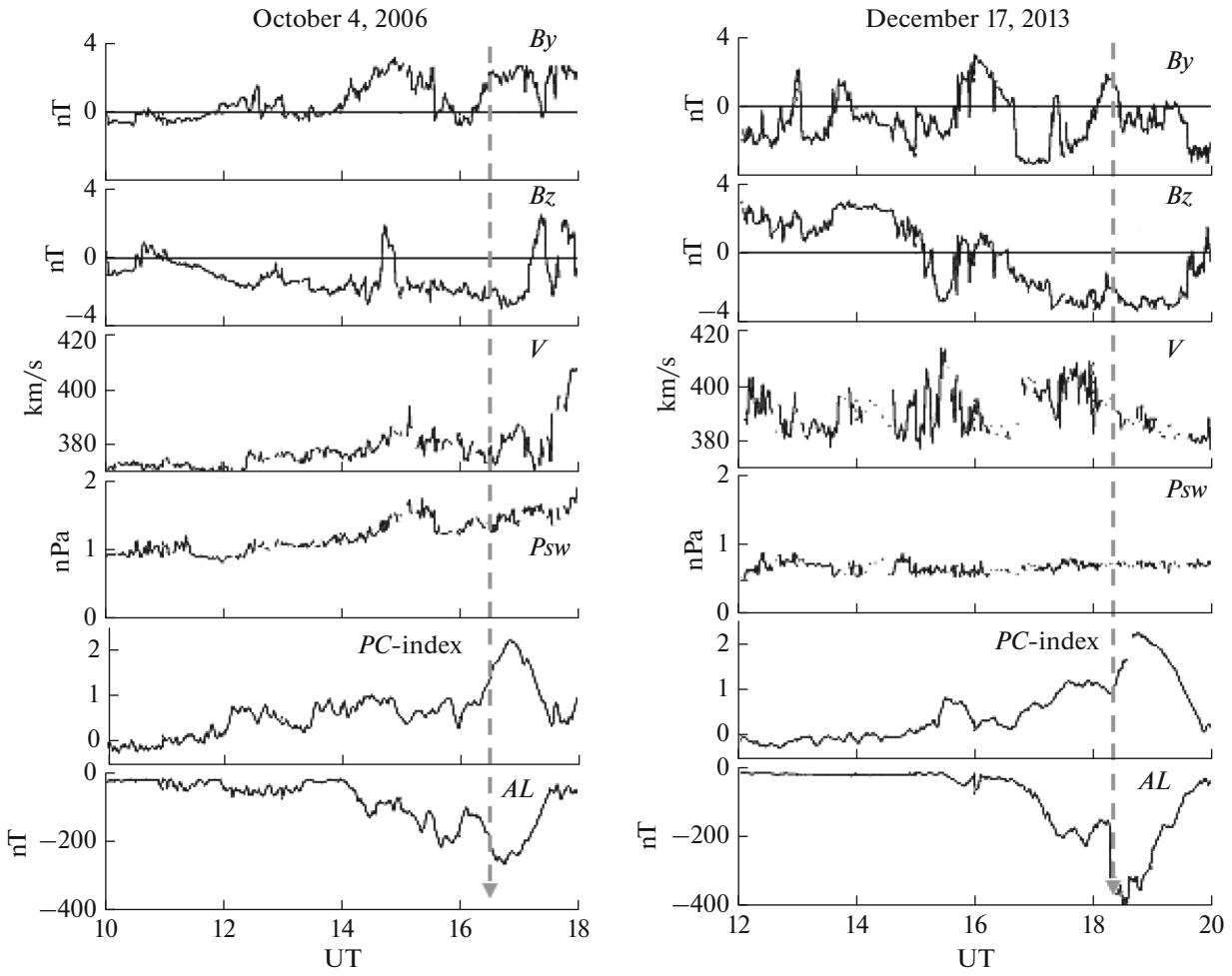

Fig. 8. Variations in IMF and solar wind parameters according to OMNI data during the discussed events. The vertical dashed line shows the onset time of the polar substorms.

tive magnetic bays in the region of a contracted auroral oval, i.e., at latitudes above ~70° MLAT; (2) maximum occurrence in the earlier pre-midnight hours of local geomagnetic time; (3) generation only at low solar wind speeds; and (4) development under magnetically quiet or weakly disturbed geomagnetic conditions.

Thus, we can conclude that polar substorms are a specific type of "classical" substorm and are a characteristic disturbance that develops under conditions of a constracted auroral oval, i.e., on more distant *L*-shells compared to "classical" substorms.

ACKNOWLEDGMENTS

The authors are grateful to the creators of the OMNI database (http://omniweb.gsfc.nasa.gov), SuperMAG databases (https://supermag.jhuapl.edu/), IMAGE (http://space.fmi.fi/image/) and AMPRE (https://ampere.jhuapl.edu/browse/) for their use in the work.

FUNDING

The work of N.G. Kleimenova and L.M. Malysheva was supported by the state task of the IPE RAS, that of L.I. Gromova and S.V. Gromov was supported by the state task of IZMIRAN, and that of I.V. Despirak and A.A. Lyubchich was supported by the state task of the PGI.

CONFLICT OF INTEREST

The authors declare that they have no conflicts of interest.

REFERENCES

Akasofu, S.-I., The development of the auroral substorm, *Planet. Space Sci.*, 1964, vol. 12, no. 4, pp. 273–282. https://doi.org/10.1016/0032-0633(64)90151-5

Akasofu, S.-L., Perreault, P.D., Yasuhara, F., and Meng, C.-I., Auroral substorms and the interplanetary magnetic field, *J. Geophys. Res.*, 1973, vol. 78, no. 31, pp. 7490–7508. https://doi.org/10.1029/JA078i031p07490

Akasofu, S.-I., Where is the magnetic energy for the expansion phase of auroral substorms accumulated? 2. The main body, not the magnetotail, *J. Geophys. Res.: Space Phys.*, 2017, vol. 122, pp. 8479–8487. https://doi.org/10.1002/2016JA023074

Anderson, B.J., Takahashi, K., Kamei, T., Waters, C.L., and Toth, B.A., Birkeland current system key parameters derived from iridium observations: Method and initial validation results, *J. Geophys. Res.*, 2002, vol. 107, p. 1079. https://doi.org/10.1029/2001JA000080

Antonova, E.E., Vorobjev, V.G., Kirpichev, I.P., Yagodkina, O.I., and Stepanova, M.V., Problems with mapping the auroral oval and magnetospheric substorms, *Earth Planets Space*, 2015, vol. 67, p. 166. https://doi.org/10.1186/s40623-015-0336-6

Antonova, E.E., Stepanova, M., Kirpichev, I.P., et al., Structure of magnetospheric current systems and mapping of high latitude magnetospheric regions to the ionosphere, *J. Atmos. Sol.-Terr. Phys.*, 2016, vol. 177, pp. 103–114. https://doi.org/10.1016/j.jastp.2017.10.013

Antonova, E.E., Stepanova, M.V., and Kirpichev, I.P., Main features of magnetospheric dynamics in the conditions of pressure balance, *J. Atmos. Sol.-Terr. Phys.*, 2023, vol. 242. https://doi.org/10.1016/j.jastp.2022.105994

Clausen, L.B.N., Baker, J.B.H., Ruohoniemi, J.M., Milan, S.E., and Anderson, B.J., Dynamics of the region 1Birkeland current oval derived from the Active Magnetosphere and Planetary Electrodynamics Response Experiment (AMPERE), *J. Geophys. Res.*, 2012, vol. 117, A06233. https://doi.org/10.1029/2012JA017666

Despirak, I.V., Lyubchich, A.A., Biernat, H.K., and Yahnin, A.G., Poleward expansion of the westward electrojet depending on the solar wind and IMF parameters, *Geomagn. Aeron. (Engl. Transl.)*, 2008, vol. 48, no. 3, pp. 284–292.

Despirak, I.V., Lyubchich, A.A., and Kleimenova, N.G., Polar and high latitude substorms and solar wind conditions, *Geomagn. Aeron. (Engl. Transl.)*, 2014, vol. 54, no. 5, pp. 575–582. https://doi.org/10.1134/S0016793214050041

Despirak, I.V., Lubchich, A.A., and Kleimenova, N.G., High-latitude substorm dependence on space weather conditions in solar cycle 23 and 24 (SC23 and SC24), *J. Atmos. Sol.-Terr. Phys.*, 2018, vol. 177, pp. 54–62. https://doi.org/10.1016/j.jastp.2017.09.011

Despirak, I.V., Lyubchich, A.A., and Kleimenova, N.G., Supersubstorms and conditions in the solar wind, *Geomagn. Aeron. (Engl. Transl.)*, 2019, vol. 59, no. 2, pp. 170–176. https://doi.org/10.1134/S0016793219020075

Despirak, I.B., Kleimenova, N.G., Lyubchich, A.A, Malysheva, L.M., Gromova, L.I., Roldugin, A.V., and Kozelov, B.V., Magnetic Substorms and Auroras at the Polar Latitudes of Spitsbergen: Events of December 17, 2012, *Bull. Russ. Acad. Sci.: Phys.*, 2022, vol. 86, no. 3, pp. 266–274. https://doi.org/10.3103/S1062873822030091

Dmitrieva, N.P. and Sergeev, V.A., Appearance of an auroral electrojet at polar cap latitudes: characteristics of the phenomenon and the possibility of its use for diagnostics of large-scale high-speed solar wind streams, *Magnitos. Issled.*, 1094, no. 3, pp. 58–66.

Fel'dshtein, Ya.I., Some problems of the morphology of polar glow and magnetic disturbances at high latitudes, *Geomagn. Aeron.*, 1963, vol. 3, no. 2, pp. 227–239.

Feldstein, Y.I. and Starkov, G.V., Dynamics of auroral belt and geomagnetic disturbances, *Planet. Space Sci.*, 1967, vol. 15, pp. 209–229. https://doi.org/10.1016/0032-0633(67)90190-0

Frey, H.U., Mende, S.B., Angelopoulos, V., and Donovan, E.F., Substorm onset observations by IMAGE-FUV, *J. Geophys. Res.*, 2004, vol. 109, A10304. https://doi.org/10.1029/2004JA010607

Hones, E.W., The poleward leap of the auroral electrojet as seen in auroral images, *J. Geophys. Res.*, 1985, vol. 90, pp. 5333–5337. https://doi.org/10.1029/JA090iA06p05333

Hones, E.W., Akasofu, S.-I., Jr., Bame, S.J., and Singer, S., Poleward expansion of the auroral oval and associated phenomena in the magnetotail during auroral substorms, 2, *J. Geophys. Res.*, 1971, vol. 76, pp. 8241–8257. https://doi.org/10.1029/JA076i034p08241

Horning, B.L., McPherron, R.L., and Jackson, D.D., Application of linear inverse theory to a line current model of substorm current systems, *J. Geophys. Res.*, 1974, vol. 9, no. 34, pp. 5202–5210. https://doi.org/10.1029/JA079i034p05202

Iijima, T. and Potemra, T.A., Large-scale characteristics of field aligned currents associated with substorms, *J. Geophys. Res.*, vol. 83, no. 2, pp. 599–615. https://doi.org/10.1029/JA083iA02p00599

Keiling, A. and Takahashi, K., Review of Pi2 models, *Space Sci. Rev.*, 2011, vol. 161, pp. 63–148.

Kepko, L., McPherron, R.L., Amm, O., et al., Substorm current wedge revisited, *Space Sci. Rev.*, 2015, vol. 190, pp. 1–46. https://doi.org/10.1007/s11214-014-0124-9

Kleimenova, N.G., Antonova, E.E., Kozyreva, O.V., Malysheva, L.M., Kornilova, T.A., and Kornilov, I.A., Wave structure of magnetic substorms at high latitudes, *Geomagn. Aeron. (Engl. Transl.)*, 2012, vol. 52, no. 6, pp. 746–754. https://doi.org/10.1134/S0016793212060059

Loomer, E.I. and Gupta, J.C., Some characteristics of high latitude substorms, *J. Atmos. Terr. Phys.*, 1980, vol. 42, pp. 645–652.

Lui, A.T.Y., Perreault, P.D., Akasofu, S.-I., and Anger, C.D., The diffuse aurora, *Planet. Space Sci.*, 1973, vol. 21, no. 5, pp. 857–861. https://doi.org/10.1016/0032-0633(73)90102-5

Lui, A.T.Y., Akasofu, S.-I., Hones, E.W., Jr., Bame, S.J., and McIlwain, C.E., Observation of the plasma sheet during a contracted oval substorm in the prolonged quiet period, *J. Geophys. Res.*, 1976, vol. 81, no. 7, pp. 1415–1419. https://doi.org/10.1029/JA081i007p01415

McPherron, R.L., Russell, C.T., and Aubry, M.P., Satellite studies of magnetospheric substorms on August 15, 1968: 9. Phenomenological model for substorms, *J. Geophys.*

Res., 1973, vol. 78, no. 16, pp. 3131–3149. https://doi.org/10.1029/ja078i016p03131.

Mende, S.B., Frey, H.U., Geller, S.P., and Doolittle, J.H., Multi-station observations of auroras: Polar cap substorms, *J. Geophys. Res.*, 1999, vol. 104, no. A2, pp. 2333–2342. https://doi.org/10.1029/1998JA900084

Mende, S.B., Heetderks, H., Frey, H.U., et al., Far ultraviolet imaging from the image spacecraft.1. System design, *Space Sci. Rev.*, 2000, vol. 91, pp. 243–270.

Milan, S.E., Boakes, P.D., and Hubert, B., Response of the expanding/contracting polar cap to weak and strong solar wind driving: implications for substorm onset, *J. Geophys. Res.*, 2008, vol. 113, A09215. https://doi.org/10.1029/2008JA013340

Milan, S.E., Grocott, A., and Hubert, B., A superposed epoch analysis of auroral evolution during substorms: Local time of onset region, *J. Geophys. Res.*, 2010, vol. 115, A00I04. https://doi.org/10.1029/2010JA015663

Newell, P.T., Feldstein, Y.I., Galperin, Y.I., and Meng, C.-I., Morphology of night-side precipitation, *J. Geophys. Res.*, 1996, vol. 101, 10737–10748. https://doi.org/10.1029/95JA03516

Nielsen, E., Bamber, J., Chen, Z.-S., Brekke, A., Egeland, A., Murphree, J.S., Venkatesan, D., and Axford, W.I., Substorm expansion into the polar cap, *Ann. Geophys.*, 1988, vol. 6, no. 5, pp. 559–572.

Olson, J.V., Pi2 pulsations and substorm onsets: A review, *J. Geophys. Res.*, 1999, vol. 104, pp. 17499–17520.

Pashin, A.B., Glabmeier, K.H., Baumjohann, W., Raspopov, O.M., Yahnin, A.G., Opgenoorth, H.J., and Pellinen, R.J., Pi2 magnetic pulsations, auroral breakups, and the substorm current wedge: A case study, *J. Geophys.*, 1982, vol. 51, pp. 223–233.

Pudovkin, M.I., Raspopov, O.M., and Kleimenova, N.G., *Vozmushcheniya elektromagnitnogo polya Zemli* (Disturbances in the Earth's Electromagnetic Field), vol. 2: *Korotkoperiodicheskie kolebaniya geomagnitnogo polya* (Short-Period Oscillations in the Geomagnetic Field), Leningrad: LGU, 1976.

Pytte, T., McPherron, R.L., Kivelson, M.G., Wes, H.I., Jr., and Hones, E.W., Multiple-satellite studies of magnetospheric substorms: Plasma sheet recovery and the poleward leap of auroral zone activity, *J. Geophys. Res.*, 1978, vol. 83, pp. 5256–5268. https://doi.org/10.1029/JA083iA11p05256

Safargaleev, V.V., Mitrofanov, V.M., and Kozlovskii, A.E., Complex analysis of the polar substorm based on magnetic, optical, and radar observations near Spitsbergen, *Geomagn. Aeron. (Engl. Transl.)*, 2018, vol. 58, no. 4, pp. 793–808. https://doi.org/10.1134/S0016793218040151

Safargaleev, V.V., Kozlovsky, A.E., and Mitrofanov, V.M., Polar substorm on 7 December 2015: Preonset phenomena and features of auroral breakup, *Ann. Geophys.*, 2020, vol. 38, no. 4, pp. 901–918. https://doi.org/10.5194/angeo-38-901-2020

Saito, T., Geomagnetic pulsations, *Space Sci. Rev.*, 1969, vol. 10, pp. 319–412. https://doi.org/10.1007/BF00203620

Saito, T., Yumoto, K., and Koyama, Y., Magnetic pulsation *Pi*2 as a sensitive indicator of magnetospheric substorm, *Planet. Space Sci.*, 1976, vol. 24, pp. 1025–1029.

Sergeev, V.A., On the longitudinal localization of the substorm active region and its changes during the substorm, *Planet. Space Sci.*, 1974, vol. 22, pp. 1341–1343.

Sergeev, V.A., Yahnin, A.G., Dmitrieva, N.P., Substorms in the polar cap: The effect of high-speed streams of the solar wind, *Geomagn. Aeron.*, 1979, vol. 19, no. 6, pp. 1121–1122.

Troitskaya, V.A. and Kleimenova, N.G., Micropulsations and VLF-emissions during substorms, *Planet. Space Sci.*, 1972, vol. 20, no. 9, pp. 1499–1519. https://doi.org/10.1016/0032-0633(72)90053-0

Troshichev, O. and Janzhura, A., Relationship between the PC and AL indices during repetitive bay-like magnetic disturbances in the auroral zone, *J. Atmos. Sol.-Terr. Phys.*, 2009, vol. 71, pp. 1340–1352.

Troshichev, O.A., Kuznetsov, B.M., and Pudovkin, M.I., The current systems of the magnetic substorm growth and explosive phases, *Planet. Space Sci.*, 1974, vol. 22, pp. 1403–1412.

Troshichev, O.A., Podorozhkina, N.A., Sormakov, D.A., and Janzhura, A.S., PC index as a proxy of the solar wind energy that entered into the magnetosphere: Development of magnetic substorms, *J. Geophys. Res.: Space Phys.*, 2014, vol. 119, no. 8, pp. 6521–6540. https://doi.org/10.1002/2014JA019940

Zverev, V.A., Loginov, G.A., Pudovkin, M.I., and Raspopov, O.M., The behavior of pulsations of the geomagnetic field in the period preceding polar geomagnetic disturbances, *Geomagn. Issled.*, 1969, no. 11, pp. 37–44.